Journal of Archaeological Science: Reports 58 (2024) 104708

Contents lists available at ScienceDirect

Journal of Archaeological Science: Reports

journal homepage: www.elsevier.com/locate/jasrep

Decoding Capua's roof terracotta: A multi-analytical study of the *Fondo Patturelli* sanctuary and *Alveo Marotta* furnace (6th century BCE – 1st century BCE)

Maria Verde [a,*], Alberto De Bonis [b,c,*], Natalie Wagner [d,e,f], Francesca d'Aniello [b], Vincenzo Morra [b]

[a] Dipartimento di Architettura (DiARC), Università degli Studi di Napoli Federico II, Via Forno Vecchio, 36, 80134 Naples, Italy
[b] Dipartimento di Scienze della Terra, dell'Ambiente e delle Risorse (DiSTAR), Università degli Studi di Napoli Federico II, Naples, Italy
[c] CRACS, Center for Research on Archaeometry and Conservation Science, Via Cintia 21, 80126 Naples, Italy
[d] Deutsches Archäologisches Institut, Rome, Italy
[e] Dipartimento di Lettere e Beni Culturali, Università degli Studi della Campania Luigi Vanvitelli, Santa Maria Capua Vetere, Italy
[f] Humboldt-Universität zu Berlin, Germany

ARTICLE INFO

Keywords:
Architectural terracotta
Capua
Archaeometric investigation
Provenance
Pyrotechnology

ABSTRACT

The main focus of this study was to examine 25 samples of archaeological ceramic materials currently preserved in the Archaeological Museum of the Ancient Capua and Mitreo investigated in the framework of an international project. These samples primarily consist of architectural terracotta from the *Fondo Patturelli* extra-urban sanctuary, as well as architectural terracotta, pottery and waste material from the nearby *Alveo Marotta* furnace.

To investigate these artifacts, a multi-analytical mineralogical-petrographic approach was performed. Thin section observations revealed that almost all samples exhibit a coarse-grained paste. The fragments were categorized into three petrographic groups based on the type and quantity of temper, which is mostly composed of volcanic grains. They include lithics and juvenile fragments (obsidians and pumices) ascribed to the products of the major Campanian eruptions as detected via FESEM-EDS. Bulk chemical analyses (WD-XRF) show that almost all samples form a homogeneous group made with Ca-rich clayey raw materials, also including three wastes of tiles from the *Alveo Marotta*. By contrast, other two wastes from *Alveo Marotta* were produced with Ca-poor clay suggesting the use of a different raw material.

From a technological point of view the samples are characterized by a thermal range that varies from 750 to 900 °C, notably different between the earlier and later production periods, with the former fired at lower temperatures.

1. Introduction and historical background

The ancient city of Capua, known today as Santa Maria Capua Vetere, is located at the foot of Mount Tifata, near the Volturno River (Fig. 1). Capua played a pivotal role as one of the most important inland transportation hubs in southern Italy. Its central location was attributed to the Via Appia, which has connected Rome and Capua since 312 BCE. This significant road, which extended to Brundisium in the 2nd century BCE, promoted the movement and interaction of people, ideas, and cultural influences between Capua and other regions. Therefore, Capua occupied a prominent position in the connectivity and cultural dynamics of the region, which is reflected in the artistic expressions and cultural exchanges of the time. Fertile fields that enabled high agricultural production, coupled with high-quality craftsmanship and artistry, contributed to the city's economic wealth (Cerchiai, 1995). The largest complex of architectural terracotta investigated in this study comes from the extramural sanctuary called *Fondo Patturelli*, presently situated in the municipality of Curti and historically located beyond the city walls of Capua (Rescigno, 2009). In the excavation campaigns conducted during the 19th and 20th centuries (Sampaolo, 2011), a plethora of artifacts was unearthed, including architectural elements (Wolf, 2023), a multitude of matronal tuff statues *Madri* (Petrillo, 2016; Haase, 2020), Oscan

* Corresponding authors at: Dipartimento di Scienze della Terra, dell'Ambiente e delle Risorse, Università degli Studi di Napoli Federico II, Naples, Italy (A. De Bonis).
E-mail addresses: maria.verde@unina.it (M. Verde), alberto.debonis@unina.it (A. De Bonis).

https://doi.org/10.1016/j.jasrep.2024.104708
Received 23 February 2024; Received in revised form 22 July 2024; Accepted 22 July 2024
Available online 29 July 2024

inscribed steles called *Iovilas* (Franchi De Bellis, 1981), votive terracottas (Migliore, 2011), and ceramics (Minoja, 2006). Most of the discovered material consisted of architectural roof tiles, primarily found in votive deposits (Koch, 1912; Rescigno and Sampaolo, 2005; Rescigno, 2009; Wagner, in press). The abundant finds from *Fondo Patturelli* are now distributed among various museums across Europe. The Museo Campano in Capua holds the largest portion of the archaeological remains from these early excavations. Additionally, artifacts from the excavations carried out by the Soprintendenza are housed in the Archaeological Museum of Ancient Capua and Mitreo.

Approximately 500 m north of the extramural sanctuary of *Fondo Patturelli*, a terracotta workshop was identified as early as 1893 (Koch, 1907). This area, known as *Alveo Marotta*, became the subject of scientific investigations in the 1980s, revealing an archaic craftsman's quarter and several kilns. One kiln with a rectangular floor plan is particularly well-preserved. These kilns were intended for various purposes, including the production of architectural terracotta, as evidenced by the in-situ discovery of semi-finished pieces, and firing failures. Around 470 BCE, the site was abandoned, followed by subsequent phases (Allegro, 1984; Allegro and Svanera, 1996).

The main objective of this study is to determine the production locations of the material, as well as making some technical observations, and to conduct a comprehensive analysis of the architectural terracotta from the ancient Capua. The archaeometric approach, undertaken as an integral component of this research endeavor, was designed to ascertain the origins and production techniques employed in the creation of these remarkable cultural heritage materials.

Suitable reference materials such as misfirings or material found inside pottery kilns are required in order to determine the origin of the samples. For this reason, the international team selected a total of 25 fragments from different time periods, either from the *Alveo Marotta* terracotta workshop or the extramural sanctuary of *Fondo Patturelli*. To facilitate a more comprehensive comparison, both ceramic fragments and misfirings of architectural terracotta were subjected to archaeometric analysis (Fig. 2).

2. Brief geological remarks

Fondo Patturelli and *Alveo Marotta* are located in Santa Maria Capua Vetere, which corresponds to ancient Capua, in the northern sector of Piana Campana (South Italy, Fig. 1). The origin of Piana Campana is closely linked to the extensional tectonics that have affected the Tyrrhenian area since the Plio-Pleistocene period (Vitale and Ciarcia, 2018; Di Girolamo and Stanzione,1973; Rolandi et al., 2003; D'Argenio et al., 2012). These tectonic processes are a response to the complex geodynamic events that have shaped the western Mediterranean region, resulting in the formation of the Tyrrhenian Basin and the Apennine-Maghreb chain (Fedele et al., 2011). The extensional tectonics caused the subsidence of the Apennines towards the central Tyrrhenian region (D'Argenio et al., 2012), leading to the sinking of the western margin and the subsequent volcanic activity (such as Roccamonfina, Phlegraean Fields, and Somma-Vesuvius) as well as the development of large depressions like Piana Campana and Piana del Sele, which were filled with volcanoclastic and alluvial sediments (Ciarcia and Vitale, 2013). Specifically, in the northern region, volcanic activity is dominated by the Roccamonfina volcano, while in the southern region, it is dominated by the Phlegraean Fields and Somma-Vesuvius.

Volcanic activity in the region began approximately 700 ka ago with the Roccamonfina volcano in the northern part of the region, followed by the Ischia Island around 150 ka ago, and subsequently, the Phlegraean Fields approximately 60 ka ago. The most recent volcanic activity occurred with the formation of the Somma-Vesuvius volcano around 25 ka ago, situated along the central sector of the Tyrrhenian margin in the region.

During the Quaternary period, these lowered areas, along with other intermontane depressions, were filled with alluvial and volcanic deposits, giving rise to the present-day Campanian, Sele River, and Tanagro River alluvial plains. The tectonic structures in the region are overlain by unconformable layers of Mio-Pliocene wedge top basin deposits of detrital origin, as well as Quaternary post-orogenic sediments and volcanic materials (Vitale and Ciarcia, 2018; Ascione et al., 2012).

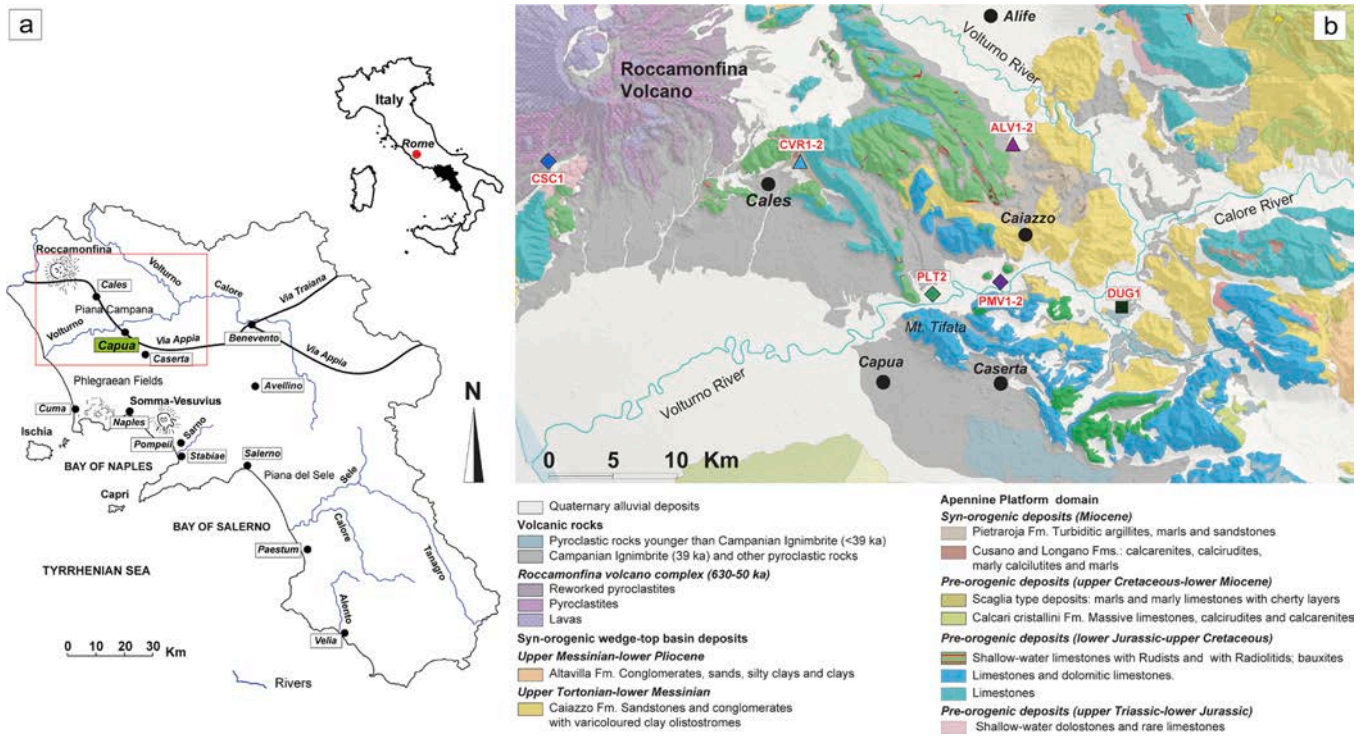

Fig. 1. (a) location of the study area. (b) geological map of the northern campania sector modified after Vitale and Ciarcia (2018) with the location of the selected samples of raw materials.

Fig. 2. The 25 samples under study divided according to the production period. The chronological framework of this study is based on the research conducted by N. Wagner (in press). Scale bar: 10 cm.

3. Materials and methods

This study focuses on twenty-five fragments of architectural terracotta and pottery (Fig. 2), which were carefully selected to cover a chronological period ranging from the 6th century BCE to the 1st century BCE. The selected samples can be divided as follows:

- 6th – 5th century BCE: Five samples from this time frame were identified (AM25 from *Alveo Marotta* and FP6, FP17, FP18, FP19 from *Fondo Patturelli*).
- 4th – 3rd century BCE: Eleven samples from the extramural sanctuary of Fondo *Patturelli* were selected for this period (FP7, FP11, FP12, FP13, FP14, FP15, FP20, FP21, FP22, FP23, FP24).
- 3rd – 2nd century BCE: One sample, FP16, was chosen from the extramural sanctuary of *Fondo Patturelli* for this period.
- 2nd – 1st century BCE: Two samples, FP9 and FP10 from the extramural sanctuary of *Fondo Patturelli*, belong to this period.
- Unknown chronology: This category includes six samples, AM1, AM2, AM3, AM4, AM5 from *Alveo Marotta*, and FP8 from *Fondo Patturelli*, which cannot be dated precisely and fall within a broad chronological span from the 6th to the 1st century BCE. They were selected as two of them (AM1, AM4) are kiln wastes, whereas AM2, AM3, and AM5 are pottery fragments investigated to compare their compositional features with architectural terracottas.

A multi-analytical approach was performed for the investigation. Macroscopic features included color of ceramic body of the specimens evaluated via a visual comparison via the Munsell Soil Colour Chart and hardness (Williams, 1990). Subsequently, minero-petrographic and chemical analyses were performed on the 25 selected samples found in the two different context, 19 samples from *Fondo Patturelli* and 6 samples from *Alveo Marotta*. The analyses mentioned below were performed at the Department of Earth, Environmental and Resources Sciences (DiSTAR) of the University of Naples Federico II.

Petrographic and textural features were investigated by means of PLM (polarized light microscopy) in thin section using a OPTIKA V-600 POL microscope connected to a ZEISS Axiocam 105 color camera (ZEN 2.3 Lite software). The abundance, size range, and angularity of the inclusions were described (e.g., Whitbread, 1995; Quinn, 2013) and evaluated by a comparator chart (Terry and Chilingar, 1995).

Bulk mineralogical composition was determined by semiquantitative X-ray powder diffraction (XRPD) using a Bruker D2 Phaser second-gen diffractometer (CuKα radiation, operating at 30 kV, 10 mA, scanning interval 4-70° 2θ, using a step interval of 0.020° 2θ, with a step counting time of 66 s, Lynxeye 1D model detector), equipped with Diffract V6 5.0 data collector software (Bruker).

Microstructural observations of the fragments in fresh fracture were performed via Scanning Electron Microscopy (SEM; JEOL 5310 instrument) and via Field Emission Scanning Electron Microscopy (FESEM; Zeiss Merlin VP Compact) to define the degree of sintering which develop in the ceramic bodies according to the different firing temperatures of the ceramic bodies (Maniatis and Tite, 1981). This analysis was carried out on 13 representative samples, chosen based on their petrographic features and mineralogical assemblage. Quantitative

microchemical analysis of mineral grains and neoformed phases in the ceramic bodies was performed on polished thin sections (carbon coated) using the FESEM; Zeiss Merlin VP Compact instrument fitted with an energy dispersive X-ray spectrometer (EDS) and Oxford Instruments Microanalysis Unit (X Max 50 EDS detector operating at 15 kV primary beam voltage, 115–125 μA filament current, and 60 μm spot size, acquisition time 10 s). The data were processed with an INCA Xstream pulse processor. The mineral standards used are reported in Guarino et al. (2021a). Precision and accuracy of EDS analysis is reported in Rispoli et al. (2019).

The bulk chemical composition of the samples was carried out on pressed powder pellets via Wavelength Dispersive X-Ray fluorescence spectrometry (WD-XRF; AXIOS PANalytical Instrument), expressed by the concentration of 10 major oxides (SiO_2, TiO_2, Al_2O_3, Fe_2O_3, MnO, MgO, CaO, Na_2O, K_2O, P_2O_5 in wt.%) and 10 trace elements (Rb, Sr, Y, Zr, Nb, Ba, Cr, Ni, Sc, V in ppm). The analytical uncertainty was of 1–2 % for the major elements and 5–10 % for trace elements (Cucciniello et al., 2017). The standards employed are described in Guarino et al. (2021b).

4. Results and discussion

4.1. Petrographic and microchemical features

The investigated samples basically show similar compositional features. However, three petrographic groups were identified based on differences related to inclusion amount and presence of specific minerals in some samples.

The first group is composed of twenty samples: AM25, FP6, FP17, FP18, FP19 (6th – 5th century BCE); FP7, FP11, FP12, FP13, FP15, FP20, FP21, FP22, FP23, FP24 (4th – 3rd century BCE), FP9, FP10 (2nd – 1st century BCE), FP16 (3rd –2 nd century BCE); AM4, FP8 (undated). The samples of this group are mostly characterized by a variable color of the ceramic body that varies from reddish to dark gray (Table 1). The optical activity of the clay matrix varies from active to inactive. Packing of the aplastic inclusions range from 25 to 30 % and show a bimodal grain size distribution (Fig. 3a-f).

The fine fraction (generally < 50 μm) is composed by tiny quartz crystals and sporadic mica. The coarse fraction (generally > 200 μm) consists of feldspars, which were identified via the microchemical analysis as sanidine ($Ab_{7-34}An_{0-6}Or_{62-93}$, Table S1, Fig. 4a) and plagioclase classified as bytownite ($Ab_{8-21}An_{76-91}Or_{1-3}$, Table S1, Fig. 4a). Clinopyroxene represented by diopside ($Wo_{46-51}En_{16-49}Fs_{4-29}$, Table S2, Fig. 4b) was also identified, along with mica and volcanic lithics characterized by evident trachyte fragments and juvenile volcanic fragments (pumices and obsidians). Microchemical analysis showed that juvenile fragments have a limited compositional variability and plot within the trachyandesite-trachyte and tephriphonolite-phonolite fields (Table S3). In fact, volcanic glass data plotted on the Total alkali vs. Silica diagram (Fig. 4c; Le Bas et al., 1986) used for effusive volcanic rocks and compared with literature data show that they are consistent with the products of the major Campanian eruptions (Morra et al., 2010; Fedele, 2022) ascribable to the alkaline and strongly alkaline rock series.

The second group consists of two samples from *Alveo Marotta* (AM1 and AM2, respectively) which differs from the first petrographic group by a lower percentage of aplastic inclusions. The color of the ceramic body varies from reddish yellow to dark grayish brown (Table 1).

The clay matrix is totally inactive and contains an amount of inclusions that range from 10 to 15 % and show a bimodal grain size distribution (Fig. 3g, h). The sample AM2 is characterized by a porous matrix. Pores are striated and elongated. The fine fraction (generally < 50 μm) is composed of tiny quartz crystals and sporadic mica. The sporadic coarse fraction (>200 μm) consists of alkali feldspar classified via microchemistry as sanidine ($Ab_{11-43}An_{2-9}Or_{55-86}$, Table S1, Fig. 4a), plagioclase as bytownite ($Ab_{13-20}An_{77-85}Or_{2-3}$, Table S1, Fig. 4a), and clinopyroxene classified as diopside ($Wo_{46-51}En_{29-46}Fs_{6-19}$, Table S2, Fig. 4b). Juvenile volcanic fragments (pumices and obsidians) are also present. Also in this case, microchemistry show a trachytic composition that, as already evidenced for the first petrographic group, nicely points to the use of a volcanic temper akin to products of Campanian volcanoes (Table S3, Fig. 4c).

The third group includes 3 samples (AM3, AM5 from *Alveo Marotta*, and FP14 from *Fondo Patturelli*) that differ from those of the previous two groups due to the presence of garnet. The samples of this group are characterized by a color of the ceramic body that varies from gray to very dark gray (Table 1). The optical activity of the clay matrix varies from active to inactive with an amount of inclusions that range from 20 to 25 % and a bimodal grain size distribution (Fig. 3). The fine fraction (<50 μm) is composed of tiny quartz crystals and sporadic mica. The

Table 1
Macroscopic characteristics of the 25 samples from Capua. Chronology is based on the research by N. Wagner (in press). AT, architectural terracotta; P, pottery; W, kiln waste.

Sample ID	Class	Site	Chronology (century BCE)	Wt. (g)	Zoning	Inner colour	Outer colour	Hardness
AM25	AT	*Alveo Marotta*	6th – 5th	13.51	–	7.5YR 6/2	7.5YR 6/2	hard
FP6	AT	*Fondo Patturelli*	6th – 5th	7.86	–	7.5YR 4/1	7.5YR 4/1	very hard
FP17	AT	*Fondo Patturelli*	6th – 5th	4.24	–	7.5YR 6/4	7.5YR 6/4	hard
FP18	AT	*Fondo Patturelli*	6th – 5th	4.75	–	5YR 6/6	5YR 6/6	soft
FP19	AT	*Fondo Patturelli*	6th – 5th	5.65	–	7.5YR 6/3	7.5YR 6/3	hard
FP7	AT	*Fondo Patturelli*	4th – 3rd	3.67	–	7.5YR 6/6	7.5YR 6/6	soft
FP11	AT	*Fondo Patturelli*	4th – 3rd	5.07	–	2.5 YR 6/4	2.5 YR 6/4	hard
FP12	AT	*Fondo Patturelli*	4th – 3rd	3.60	–	5YR 6/6	5YR 6/6	soft
FP13	AT	*Fondo Patturelli*	4th – 3rd	7.16	–	7.5YR 6/4	7.5YR 6/4	hard
FP14	AT	*Fondo Patturelli*	4th – 3rd	3.24	faded	10YR 4/1	10YR 6/4	hard
FP15	AT	*Fondo Patturelli*	4th – 3rd	8.06	–	10YR 6/4	10YR 6/4	hard
FP20	AT	*Fondo Patturelli*	4th – 3rd	4.45	–	7.5YR 6/4	7.5YR 6/4	soft
FP21	AT	*Fondo Patturelli*	4th – 3rd	3.5	–	7.5YR 6/4	7.5YR 6/4	hard
FP22	AT	*Fondo Patturelli*	4th – 3rd	3.86	–	7.5YR 6/4	7.5YR 6/4	hard
FP23	AT	*Fondo Patturelli*	4th – 3rd	3.55	–	7.5YR 6/6	7.5YR 6/6	hard
FP24	AT	*Fondo Patturelli*	4th – 3rd	4.70	–	5YR 6/6	5YR 6/6	soft
FP16	AT	*Fondo Patturelli*	3rd – 2nd	3.77	–	5YR 6/6	5YR 6/6	hard
FP9	AT	*Fondo Patturelli*	2nd – 1st	1.9	–	7.5YR 6/4	7.5YR 6/4	soft
FP10	AT	*Fondo Patturelli*	2nd – 1st	28.2	–	5YR 5/6	5YR 5/6	hard
AM1	W	*Alveo Marotta*	undated	6.00	–	10 YR 4/2	10 YR 4/2	hard
AM2	P	*Alveo Marotta*	undated	2.85	faded	5YR 6/6	5YR 4/2	hard
AM3	P	*Alveo Marotta*	undated	3.96	faded	10YR 3/1	10YR 3/1	hard
AM4	W	*Alveo Marotta*	undated	5.96	–	10YR 4/1	10YR 4/1	very hard
AM5	P	*Alveo Marotta*	undated	8.14	faded	5YR 5/1	5YR 3/1	hard
FP8	AT	*Fondo Patturelli*	undated	7.97	faded	7.5YR 3/1	7.5YR 6/4	soft

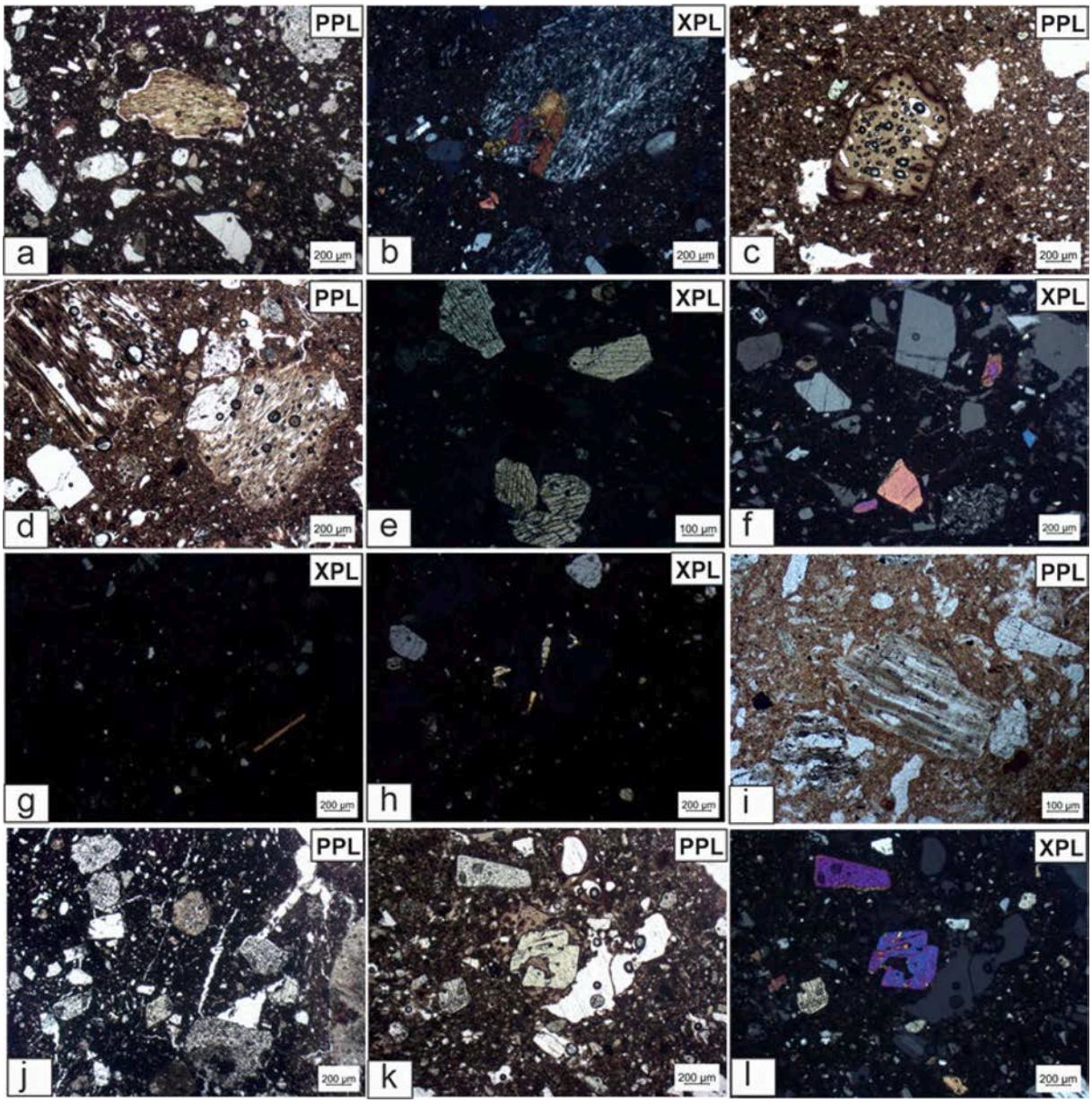

Fig. 3. Photomicrographs of some representative fragments. Petrographic group 1: (a) FP7; (b) FP10; (c) FP13; (d) FP16; (e) FP17; (f) FP24. Petrographic group 2: (g) AM1; (h) AM2. Petrographic group 3: (i) AM3; (j) AM5; (k) FP14; (l) FP14. PPL, plane polarized light; XPL, crossed polarized light.

coarse fraction (>200 μm) consists of feldspars identified via microchemical analysis as sanidine ($Ab_{14\text{-}17}An_{1\text{-}2}Or_{81\text{-}84}$, Table S1, Fig. 4a) and bytownite ($Ab_{14}An_{84}Or_2$, Table S1, Fig. 4a). Clinopyroxene classified as diopside ($Wo_{46\text{-}51}En_{30\text{-}45}Fs9\text{-}19$, Table S2, Fig. 4b) is also present, along with mica and volcanic lithics represented by evident trachyte fragments and juvenile volcanic fragments. Also in this case, juvenile fragments include pumices and obsidians that well-matches with the Campanian volcanic products, as already highlighted via microchemistry for the volcanic glasses present in samples belonging to the first and second petrographic groups (Table S3, Fig. 4c).

Garnet is present in scarce amount. Quantitative microchemistry allowed us to classify (Locock, 2008) this mineral (Table S6) as a solid solution of andradite (51.5–57.0 mol %) and grossular (26.1–29.8 mol %), a composition that well fits in with that of garnets of the Somma-Vesuvius (Scheibner et al., 2007). Specifically, this phase, associated with products of the *peri*-Vesuvian region, shows compositional features that can be ascribed to the garnets of the Avellino pumice eruption (Scheibner et al., 2007) that occurred approximately 4 k-years ago and was deposited northeast of the eruption source (Sulpizio et al., 2010). This sequence comprises five eruptive units, characterized by a prominent Plinian phase, during which around 1.5 km^3 of white to grey pumice deposits. Interestingly, the Avellino products are characterized by the presence of garnet and absence of leucite crystals, a phase that normally occurs in other products from the Somma-Vesuvius (Melluso et al., 2022) and that was not observed in the analyzed ceramic samples. Therefore, the attribution of the volcanic inclusions in the third petrographic group to the Avellino eruption is highly plausible, as these pyroclastic flow deposits extend up to 25 km from the eruption origin, which intersected the southern Caserta area (Melluso et al., 2022).

4.2. *Chemical features and sourcing of raw materials*

The chemical composition of the samples is reported in Table 2. From a chemical point of view the 20 samples of the first petrographic group also show a homogeneous bulk chemical composition in terms of major oxides and trace elements. In fact, the CaO content ranges from 7.43 to

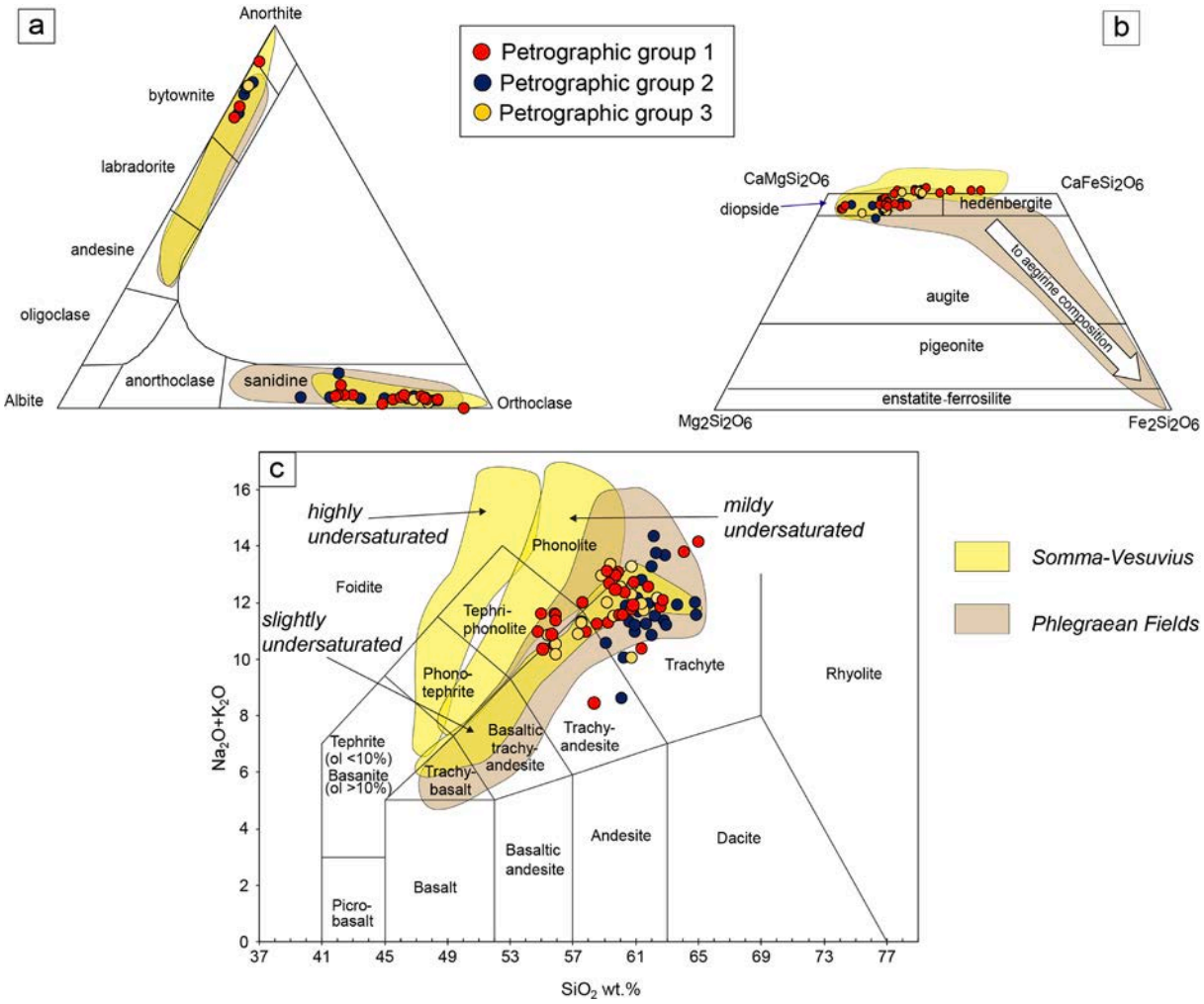

Fig. 4. Classification diagrams of the minerals and volcanic glasses micro-analyzed in some representative samples: (a) classification diagram of feldspars; (b) classification diagram of pyroxenes; (c) TAS-Total Alkali vs Silica. The compositional fields of feldspars and pyroxenes from the Phlegraean Fields (data from Melluso et al., 2012; Fedele, 2022) and Somma-Vesuvius (data from Melluso et al., 2022) are also reported, along with those of rocks and volcanic glasses (data from Morra et al., 2010).

14.5 wt.%; only one samples represented by FP8 is characterized by a slightly lower concentration of CaO (5.85 wt.%).

The analysis of major oxides (SiO_2, TiO_2, Al_2O_3, Fe_2O_3, MnO, MgO, CaO, Na_2O, K_2O, P_2O_5 in wt.%) and trace elements (Rb, Sr, Y, Zr, Nb, Ba, Cr, Ni, Sc and V in parts per million [ppm]) highlights the homogeneous chemical composition (Table 2), with a limited compositional variability in terms of both major (SiO_2 56.0–60.0 wt.%; TiO_2 0.67–0.77 wt.%; Al_2O_3 15.4–17.8 wt.%; Fe_2O_3 5.79–6.69 wt.%; MnO 0.13–0.19 wt.%; MgO 2.85–3.48 wt.%; Na_2O 0.86–1.72 wt.%; K_2O 3.04–4.86 wt.%, P_2O_5 0.19–0.47 wt.%) and trace elements. The latter, in fact, also show a good compositional homogeneity, following the behavior of major oxides (Rb 189–256 ppm, Sr 399–528 ppm, Y 32–36 ppm, Zr 235–277 ppm, Nb 25–36 ppm, Ba 572–833 ppm, Cr 89–127 ppm, Ni 45–61 ppm, Sc 15–21 ppm, V 86–119).

Some representative binary diagrams have been used to better illustrate the chemical characteristics of the ceramics (Fig. 5). To shed light on their features and the likely sources of raw materials, all the samples were compared with some Ca-rich clays (CVR1-2, ALV1-2, PLT2, PMV1) located in the northern sector of the Campania region (data from De Bonis et al., 2013 and from this study, see details in Table S4 and chemical data in Table S5). To this purpose clays from the Apennine sector belonging to the Pietraroja Formation collected in the former quarries of Calvi Risorta (CVR) and Alvignano (ALV) were selected, along with alluvial clayey sediments from the Volturnum river plain collected in the area of Pontelatone (PLT2) and Piana di Monte Verna (PMV1).

From this comparison, the samples characterized by a high-CaO character show a better affinity with the local alluvial clayey raw material represented by the Ca-rich clays of the Volturnum river plain from Pontelatone and Piana di Monte Verna, not far from Santa Maria Capua Vetere.

Regarding the samples belonging to the second petrographic group (AM1 and AM2) characterized by a lower amount of inclusions, the chemical behavior of AM1 perfectly follows the trend of the first group, both in terms of major oxides (SiO_2 56.6 wt.%; TiO_2 0.73 wt.%; Al_2O_3 16.9 wt.%; Fe_2O_3 6.46 wt.%; MnO 0.17 wt.%; MgO 2.94 wt.%; CaO 10.3 wt.%; Na_2O 1.50 wt.%; K_2O 4.08 wt.%, P_2O_5 0.25 wt.%, Table 2, Fig. 4) and trace elements (Rb 211 ppm, Sr 421 ppm, Y 35 ppm, Zr 241 ppm, Nb 33 ppm, Ba 556 ppm, Cr 104 ppm, Ni 51 ppm, Sc 20 ppm, V 119 ppm, Table 2, Fig. 5). On the other hand, the sample AM2 differs from the previously described sample; in fact, it is characterized by a lower concentration of CaO (5.95 wt.%) and higher concentrations of Al_2O_3 and Fe_2O_3 (21.84 and 8.14 wt.%, respectively). Trace elements also show compositional differences due to higher values of Y (50 ppm), Zr (435 ppm), Cr (138 ppm), Ni (70 ppm) and a lower value of Rb (317 ppm).

The chemical composition of the samples belonging to the second petrographic group were plotted on chemical binary diagrams to better

Table 2
Major (wt. %) and trace (ppm) elements composition (WD-XRF) of the investigated samples separated according to the petrographic groups.

Sample ID	Petrographic group	SiO_2	TiO_2	Al_2O_3	Fe_2O_3	MnO	MgO	CaO	Na_2O	K_2O	P_2O_5	TOT	Rb	Sr	Y	Zr	Nb	Ba	Cr	Ni	Sc	V
FP6	1st	57.7	0.70	16.4	6.00	0.16	2.96	9.89	1.72	4.24	0.21	100	230	498	33	262	32	744	97	49	19	107
FP17	1st	58.1	0.74	16.7	6.25	0.13	3.20	8.97	1.52	4.02	0.34	100	218	465	33	244	29	682	105	50	16	111
FP18	1st	58.6	0.73	17.1	6.39	0.15	3.10	7.69	1.61	4.30	0.37	100	224	475	34	252	32	688	100	46	17	107
FP19	1st	57.3	0.73	17.1	6.34	0.14	2.94	9.46	1.53	4.26	0.22	100	226	475	34	247	32	654	103	47	20	113
AM25	1st	56.8	0.74	16.9	6.38	0.17	3.16	9.70	1.35	4.43	0.30	100	205	440	34	237	31	685	117	51	16	116
FP13	1st	56.0	0.73	15.4	5.98	0.17	3.07	14.5	0.86	3.04	0.27	100	189	399	35	235	25	572	100	54	20	109
FP23	1st	56.3	0.77	16.8	6.69	0.18	3.48	10.3	1.24	3.94	0.34	100	214	489	34	250	30	754	110	57	21	110
FP24	1st	58.1	0.71	17.0	6.14	0.19	3.34	7.73	1.56	4.86	0.38	100	256	528	33	244	28	833	104	48	17	92
FP7	1st	58.5	0.75	17.4	6.34	0.16	3.21	7.49	1.47	4.38	0.30	100	234	505	32	261	31	828	127	61	18	107
FP11	1st	58.7	0.73	17.4	6.38	0.14	2.96	7.43	1.48	4.45	0.40	100	230	438	34	252	33	689	111	49	15	110
FP12	1st	57.2	0.72	16.6	6.15	0.18	3.08	10.1	1.38	4.22	0.28	100	226	493	35	270	32	752	99	49	17	106
FP15	1st	56.9	0.68	16.3	5.92	0.16	3.17	10.7	1.30	4.37	0.43	100	226	492	34	243	29	712	97	46	19	107
FP20	1st	58.7	0.67	16.2	5.79	0.17	2.93	8.75	1.57	4.72	0.47	100	227	474	34	265	31	715	89	51	19	86
FP21	1st	57.6	0.68	16.4	5.82	0.17	3.18	9.66	1.62	4.48	0.46	100	233	488	35	261	31	722	95	46	15	100
FP22	1st	57.3	0.74	17.2	6.34	0.15	2.85	8.62	1.56	4.77	0.42	100	232	499	36	267	34	709	92	45	17	103
FP16	1st	57.2	0.71	16.8	6.15	0.16	3.02	9.77	1.46	4.23	0.42	100	229	455	35	277	36	658	89	48	17	102
FP9	1st	57.2	0.74	17.1	6.51	0.16	3.09	9.21	1.44	4.11	0.41	100	224	463	34	259	34	674	105	49	18	119
FP10	1st	57.3	0.74	16.5	6.40	0.18	3.41	9.78	1.33	3.95	0.34	100	208	454	34	272	32	724	101	53	21	92
AM4	1st	56.8	0.72	16.3	6.21	0.16	3.02	11.2	1.50	3.91	0.19	100	203	435	33	241	30	618	108	52	18	118
FP8	1st	60.0	0.75	17.8	6.53	0.15	3.00	5.85	1.16	4.32	0.39	100	224	441	32	248	31	737	108	48	15	112
AM1	2nd	56.6	0.73	16.9	6.47	0.17	2.95	10.3	1.50	4.09	0.25	100	211	421	35	241	33	556	104	51	20	119
AM2	2nd	56.1	0.86	21.8	8.14	0.13	3.08	5.95	0.74	3.04	0.17	100	260	317	50	435	44	629	138	70	18	146
AM3	3rd	61.0	0.75	19.8	6.53	0.15	2.49	2.56	1.47	4.96	0.26	100	275	344	38	360	50	681	91	41	12	116
AM5	3rd	61.3	0.77	19.7	5.80	0.10	2.04	2.32	1.77	6.02	0.26	100	351	477	37	427	56	718	67	24	10	102
FP14	3rd	56.8	0.72	15.7	6.16	0.16	3.17	11.6	1.34	3.91	0.41	100	199	500	33	253	28	764	113	46	18	109

illustrate their features and the likely sources of supply of raw materials. For that reason, all the samples were compared with the same Ca-rich clay materials used for the comparison of the first group (CVR1-2, ALV1-2, PLT2, PMV1) and also with some Ca-poor clays located in the northern sector of the Campania region. These are represented by alluvial clayey sediments from the Volturnum river plain collected in the locality of Piana di Monte Verna (PMV2) and weathered pyroclastic deposits collected in the Roccamonfina volcano area (CSC1).

To sum up, AM1 shows greater affinity with the alluvial clay raw material from the Volturnum river plain (PMV1 and PLT2), as already evidenced for the first group, whereas the AM2 sample shows a chemical composition that is not akin to any of the selected raw materials. This discrepancy is significant and categorizes it as a chemical outlier.

Lastly, the analysis of major oxides and trace elements (Table 2, Fig. 5) reveals that the three ceramic samples from the third petrographic group (AM3, AM5 and FP14) exhibit a variable chemical composition. Specifically, sample FP14 from *Fondo Patturelli* shows a chemical behavior that well aligns with the first petrographic group, as does sample AM1 from the second petrographic group. This alignment is evident in both major oxides (SiO_2 56.8 wt.%; TiO_2 0.72 wt.%; Al_2O_3 15.7 wt.%; Fe_2O_3 6.16 wt.%; MnO 0.16 wt.%; CaO 11.6 wt.%; MgO 3.17 wt.%; Na_2O 1.34 wt.%; K_2O 3.91 wt.%, P_2O_5 0.41 wt.%) and trace elements (Rb 199 ppm, Sr 500 ppm, Y 33 ppm, Zr 253 ppm, Nb 28 ppm, Ba 764 ppm, Cr 113 ppm, Ni 46 ppm, Sc 18 ppm, V 109). These values are consistent with the utilization of a Ca-rich clay from the Volturno River plain, as previously hypothesized for the first group (Fig. 5).

Conversely, samples AM3 and AM5 from *Alveo Marotta* exhibit a distinct chemical composition compared to the aforementioned groups (Fig. 4), both in terms of major oxides (SiO_2 61.0–61.3 wt%; TiO_2 0.75–0.77 wt.%; Al_2O_3 19.7–19.8 wt.%; Fe_2O_3 5.80–6.53 wt.%; MnO 0.10–0.15 wt.%; MgO 2.04–2.49 wt.%; CaO 2.32–2.56 wt.%; Na_2O 1.47–1.77 wt.%; K_2O 4.96–6.02 wt.%, P_2O_5 0.26 wt.%) and trace elements (Rb 275–351 ppm, Sr 344–477 ppm, Y 37–38 ppm, Zr 360–427 ppm, Nb 50–57 ppm, Ba 681–718 ppm, Cr 67–91 ppm, Ni 24–41 ppm, Sc 10–12 ppm, V 102–116). In this case, these two samples are more compatible with the use of an alluvial raw material with a low calcium oxide concentration from the nearby Volturnum river plain.

The ternary diagram of Fig. 6 compares the samples to the reference clays and selected pottery productions from the northern Campania sector. This plot offers an additional point of view about the mix-design of the architectural terracotta from the ancient Capua. Based on a mass balance involving major oxides shown in the ternary diagram, we made a theoretical simulation of a mix (e.g., De Bonis et al., 2016) between the alluvial clay (PLT2) from the Volturno river floodplain and a volcanic temper (DUG1) from the surrounding area, both exploited for a current traditional production of bricks in the vicinity of the archaeological area. Interestingly, samples of the first petrographic group, which represent the main cluster of architectural terracotta, lie in correspondence of the mixing line approximately between the 30 and the 50 % of the volcanic temper (DUG1) added to the alluvial clay (PLT2), where a sample of a modern traditional brick made with the same raw materials also plots (Fig. 6).

As done in the binary diagrams (Fig. 5), local clays of marine origin were also plotted in Fig. 6. These raw materials were exploited for the manufacture of the large production of fine ware from Cales (Verde et al., 2023a; Guarino et al., 2011), an important production town located at ca. 20 km northwest of the investigated site. These marine clays are characterized by the presence of planktonic foraminifers, which lack in the architectural terracotta, for which we can definitively exclude the use of marine clays.

Ca-rich coarse-grained ceramics from Cales (Verde et al., 2023b) were used for comparison. They are represented by supports used as kiln furniture and a sample of dolium, which show a composition that fits with that of the architectural terracotta of the main cluster (Fig. 6).

Samples of the second petrographic group (AM1, AM2) confirm the chemical behavior described above (Fig. 5). More in details, AM1 is

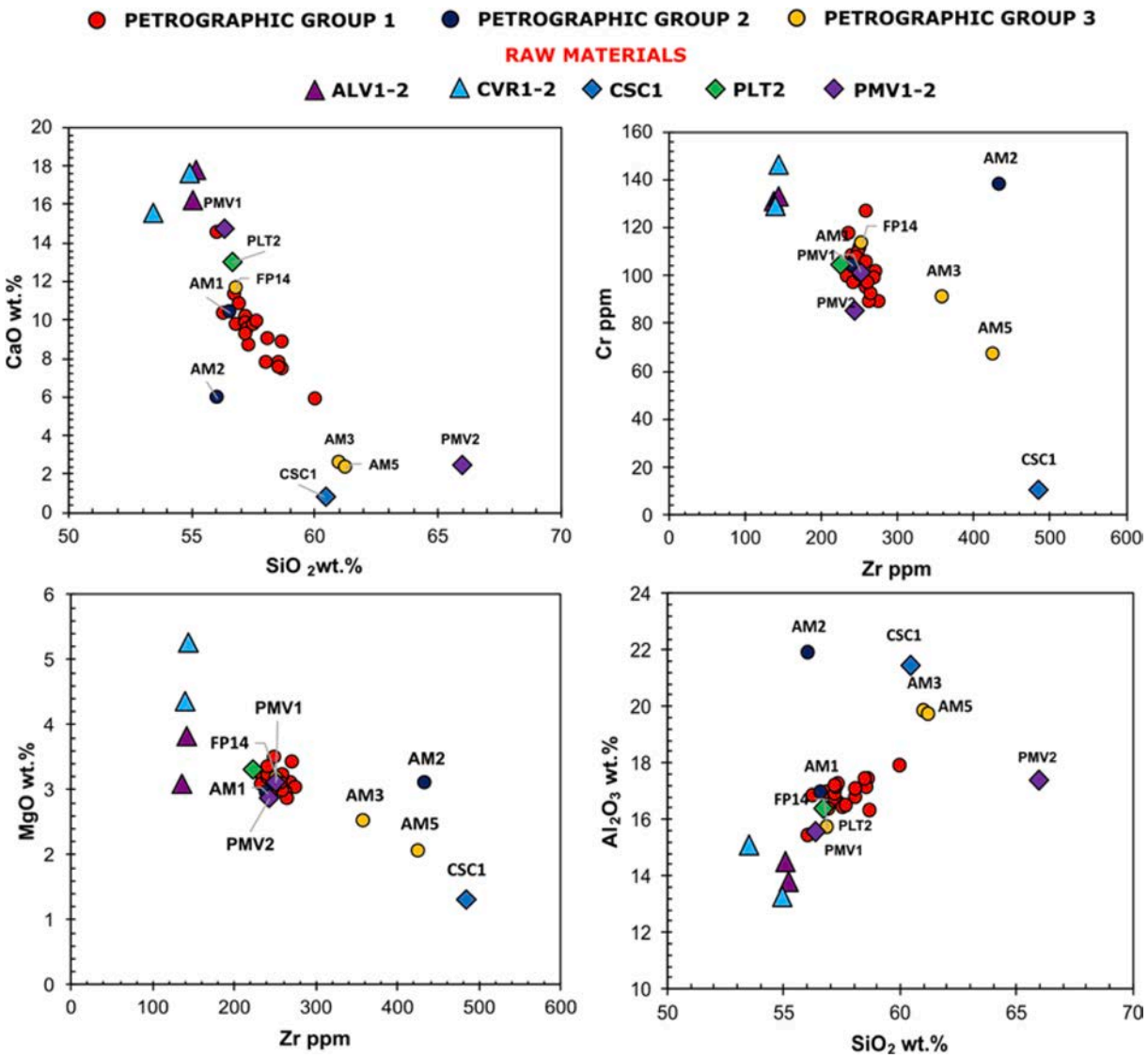

Fig. 5. WD-XRF binary diagrams with major oxides (wt.%) and trace elements (ppm) compared with low- and Ca-rich clay raw materials from the northern sector of the Campania region. Ca-poor clay raw materials = PMV2 (Piana di Monte Verna; alluvial clay); CSC1 (Cascano; weathered pyroclastic deposits). Ca-rich clay raw materials = ALV1-2 (Alvignano; marine clays); CVR1-2 (Calvi Risorta; marine clays); PLT2 (Pontelatone; alluvial clay); PMV1 (Piana di Monte Verna; alluvial clay). Data and details of clay samples are available in Tables S4 and S5.

similar to samples of the first petrographic group, whereas AM2 represents an outlier (Fig. 6). Regarding the third petrographic group, one sample (FP14) is in line with those of the main cluster. Conversely AM3 and AM5, as already evidenced in the binary diagrams of Fig. 5, show different features. In fact, they show (Fig. 6) an affinity with Ca-poor alluvial clay sediments (PMV2) from the Volturno plain influenced by a pyroclastic component (i.e., CSC1, DUG1). Similarly, Ca-poor raw materials from the surrounding area were likely exploited for pottery productions from the nearby sites (Fig. 6), which include common wares from Cales (Verde et al., 2023b) and thin-walled pottery from Alife (Grifa et al., 2015).

4.3. Pyrotecnology

Equivalent Firing Temperatures (EFTs; e.g., De Bonis et al., 2017 and references therein) were investigated via mineralogical assemblage (Table 3) related to the breakdown and neoformation of minerals upon firing and according to the method proposed by Maniatis and Tite (1981), which is based on the observation at the FESEM of typical microstructural markers. For the latter purpose, based on the mineralogical assemblage, optical features and chronologies, 13 representative samples (Table 3) of each period were selected for FESEM observation in order to define the technological changes that occurred from the 6th century BCE to the 1st century BCE.

Although from a chemical and petrographic point of view 3 groups have been recognized that do not appear to have a chronological correspondence, from a technological point of view related to firing dynamics samples belonging to the same chronology appear to have similar mineralogical and microstructural features.

As a matter of fact, the five samples ascribable to the 6th – 5th century BCE represented by FP6, FP17, FP18, and FP19 from *Fondo Patturelli*, and AM25 from *Alveo Marotta* (Table 3) show a mineralogical assemblage featured by quartz and feldspar that represent the most abundant phase, ubiquitous pyroxene from scarce to abundant, illite/mica from sporadic to frequent, and traces of calcite. Indeed, the neoformed Ca-silicates also characterize the samples and are represented by gehlenite, which start to form approximately at 800/850 °C (Cultrone et al., 2001; De Bonis et al., 2014). Neoformed iron oxides are represented by Fe^{3+} oxide (hematite) that points to a prevailing oxidizing firing atmosphere. From the intersection of the mineralogical

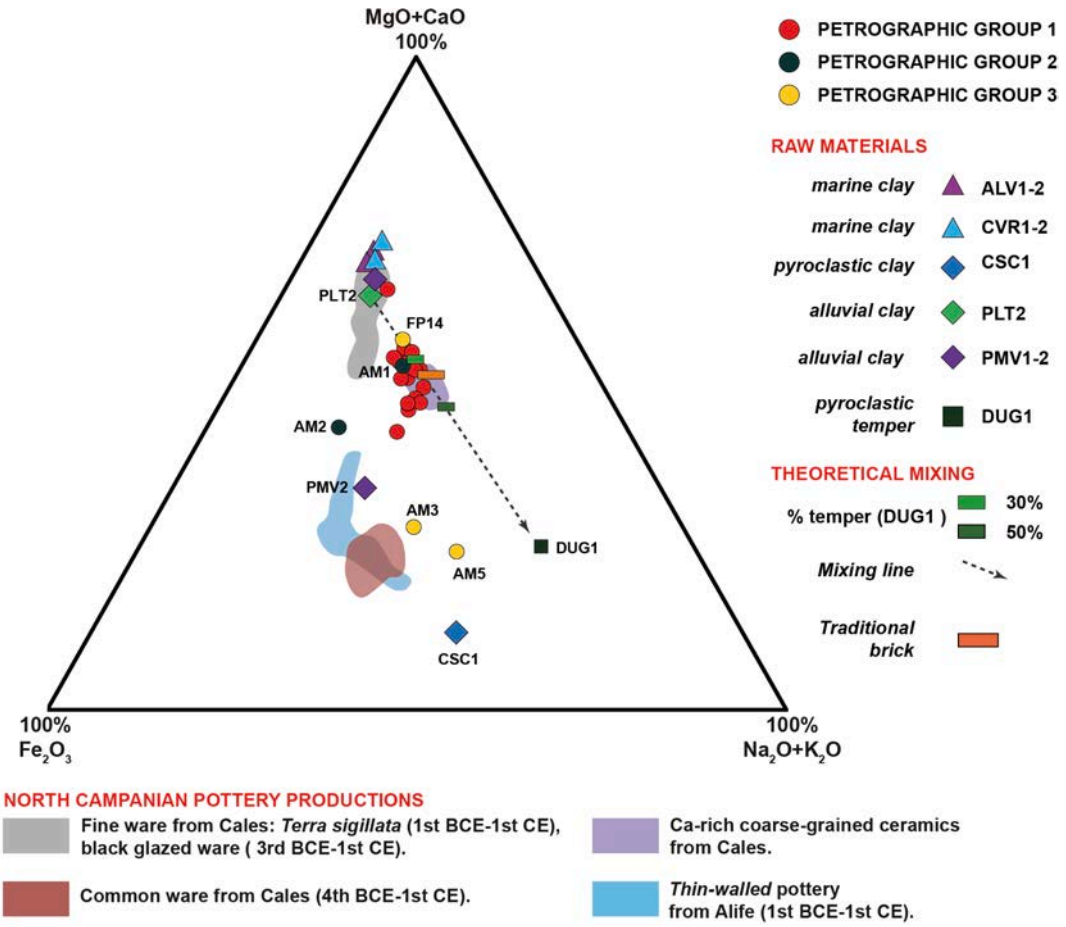

Fig. 6. Ternary diagram (modified from Vincenzini and Fiori, 1977) showing data of the samples of the petrographic groups 1, 2, and 3, compared with reference samples of clays (see description in the caption of Fig. 5) and with the compositional fields of selected pottery productions from the northern Campania sector. Reference groups of pottery include fine wares (Verde et al., 2023a; Guarino et al., 2011), common wares and coarse-grained ceramics from Cales (Verde et al., 2023b), and thin-walled pottery from Alife (Grifa et al., 2015). The theoretical mix of a local alluvial clay (PLT2) and a volcanic temper (DUG1) is reported, along with the composition of a modern traditional brick made with the same raw materials. Data and details of raw materials and modern brick samples are available in Tables S4 and S5.

assemblage and microstructural observations it was possible to estimate the EFTs. The latter vary from 800to 900 °C in FP17 (Fig. 7a) and FP18 due to the presence of an intermediate degree of sintering between an initial and an extensive vitrification stage (IV/V). In FP19 the extensive vitrification (Fig. 7b) and the remainder of illite/mica (Table 3) point to slightly higher EFTs (850–900 °C), whereas higher EFTs (1000–1100 °C) were inferred for the sample FP6 due the presence of a microstructure characterized by a continuous vitrification with coarse bloating pores (CV(CB)); Table 3, Fig. 7c), associated to the absence of illite/mica and gehlenite still present in traces (De Bonis et al., 2014).

On the contrary, the samples attributable to the 4th – 3rd century BCE represented by FP7, FP11, FP12, FP13, FP14, FP15, FP20, FP21, FP22, FP23, and FP24 exhibit a mineralogical composition characterized by quartz, feldspar, calcite, illite/mica, and pyroxene, varying from absent to frequent (Table 3). Traces of hematite were identified in FP7, FP11, FP15, FP20, FP21, FP22, FP23, and FP24 (Table 3), which indicate a prevailing use of an oxidizing atmosphere. Moreover, FP13 and FP15 revealed the presence of chlorite. The estimated firing temperatures for FP13 and FP15 are < 750 °C due to the presence of chlorite and a microstructure characterized by a non-vitrified paste (Fig. 7d; Table 3). However, in all samples of this period EFTs do not exceed 850 °C (Table 3). This is confirmed by the scarce or absence of vitrification structures detected in the representative samples of this period, along with the ubiquitous presence of the illite-like phase (Table 3); in FP20 the presence of hematite in traces suggests temperatures not lower than 750 °C (Nodari et al., 2007) and not higher than 800 °C due to an intermediate structure between no vitrification and initial vitrification (NV+; Table 3, Fig. 7e) observed in this sample. Where gehlenite was detected in traces (samples FP7, FP11, FP22) a lower temperature limit of 800 °C could be supposed. A particular condition was detected in sample FP7, where EFTs of approximately 800–850 °C were inferred due to a prevailing initial vitrification structure (Fig. 7f) spotted locally in the paste by an extensive vitrification with fine bloating pores (Fig. 7g). This is likely due to the relatively lower concentration of CaO (~7.5 wt. %) associated with a shift to reducing conditions of firing that created a state of incipient bloating (Maniatis and Tite, 1981).

Regarding the sample attributed to the 3rd – 2nd century BCE represented by FP16 (Table 3), it exhibits a mineralogy composed of quartz, feldspar, clinopyroxene, illite/mica, calcite, and traces of hematite, which is associated with an initial vitrification stage locally spotted with an extensive vitrification with fine bloating pores, thus suggesting an EFT that ranges from 800 to 850 °C. FP9 and FP10 (2nd – 1st century BCE, Table 3) show a mineralogical composition dominated by quartz and feldspar as the most abundant phases, followed by pyroxene, illite/mica, calcite, and hematite. The identification of an initial vitrification stage in FP9 (Fig. 7h) suggests equivalent firing temperatures ranging from 800 to 850 °C.

In contrast, the six samples (FP8, AM1, AM2, AM3, AM4, AM5, Table 3), for which a precise chronology is not available, but in any case fall within a broad timeframe from the 6th to the 1st century BCE, are

Table 3
Semi-quantitative mineralogical analysis (XRPD) and vitrification stage determined via SEM and FESEM* of the investigated samples separated according to the petrographic groups. xxxx = predominant; xxx = abundant; xx = frequent; x = sporadic; tr. = traces.

Sample	Petrographic group	Chronology	Qz	Fsp	Px	Cal	Gh	Ilt/mca	Hem	Others	Vitrification stage	EFTs (°C)
FP6	1st	6th – 5th century BCE	xxx	xxxx	xxx	tr.	tr.	–	tr.	–	CV(CB)	>1000
FP17	1st	6th – 5th century BCE	xxxx	xx	x	tr.	tr.	x	tr.	–	IV/V	800–900
FP18	1st	6th – 5th century BCE	xxxx	xx	x	–	tr.	x	tr.	–	IV/V*	800–900
FP19	1st	6th – 5th century BCE	xxx	xxxx	xxx	–	tr.	x	tr.	–	V	850–900
AM25	1st	6th – 5th century BCE	xxxx	xx	x	x	x	x	–	–	–	850–900
FP13	1st	4th – 3rd century BCE	xxxx	x		xxx	–	xx	–	Chl	NV	<750
FP23	1st	4th – 3rd century BCE	xxxx	xx	x	x	–	x	tr.	–	–	750–850
FP24	1st	4th – 3rd century BCE	xxxx	xxxx	xx	–	–	x	tr.	–	–	750–850
FP7	1st	4th – 3rd century BCE	xxxx	xx	xx	–	tr.	x	tr.	–	IV-V(FB)*	800–850
FP11	1st	4th – 3rd century BCE	xxxx	xx	x	–	tr.	x	tr.	–	–	800–850
FP12	1st	4th – 3rd century BCE	xxxx	xx	x	x	–	xx	–	–	–	750–850
FP15	1st	4th – 3rd century BCE	xxxx	xx	x	xx	–	xx	tr.	Chl	NV*	<750
FP20	1st	4th – 3rd century BCE	xxxx	xx	x	x	–	x	tr.	–	NV+	750–800
FP21	1st	4th – 3rd century BCE	xxxx	xx	x	tr.	–	x	tr.	–	–	750–850
FP22	1st	4th – 3rd century BCE	xxxx	xx	x	x	tr.	xx	tr.	–	–	800–850
FP16	1st	3rd – 2nd century BCE	xxxx	xx	x	x	–	x	tr.	–	IV-V(FB)*	800–850
FP9	1st	2nd – 1st century BCE	xxxx	xx	x	x	–	x	tr.	–	IV	800–850
FP10	1st	2nd – 1st century BCE	xxxx	xx	x	x	–	x	tr.	–	–	750–850
AM4	1st	undated	xxx	xxxx	xxx	–	–	–	–	–	CV(CB)*	>1050
FP8	1st	undated	xxxx	xx	x	tr.	–	xx	tr.	–	–	750–850
AM1	2nd	undated	xxx	xxxx	xx	tr.	–	x	–	–	–	850–950
AM2	2nd	undated	xxxx	xx	x	tr.	tr.	–	–	–	V	950–1050
AM3	3rd	undated	xxxx	xx	x	–	–	xx	tr.	–	–	750–850
AM5	3rd	undated	xxx	xxxx	xx	–	–	x	tr.	–	IV	750–850
FP14	3rd	4th – 3rd century BCE	xxxx	x	x	x	–	xx	–	–	–	750–850

Abbreviations: Qz = quartz; Fsp = feldspar; Px = pyroxene; Cal = calcite; Gh = gehlenite; Ilt/mca = illite/mica; Hem = hematite; Chl = chlorite; CV(CB) = continuous vitrification with coarse bloating pores; V = extensive vitrification; V(FB) extensive vitrification with fine bloating pores; IV = initial vitrification; NV = No vitrification; EFTs = Equivalent Firing Temperatures.

characterized by a mineralogy consisting of quartz, feldspar, and pyroxene; illite/mica was also identified in most samples and is frequent in FP8 and AM3 where, along with traces of hematite, indicates EFTs of approximately 750–850 °C.

AM1 is a greyish object classified as a waste and is characterized by the traces of calcite and sporadic illite/muscovite that suggest an EFT of 850–950 °C; hematite is absent likely for a reducing condition of firing. The absence of hematite was also detected in AM2, which shows a vitrified ceramic body and the total absence of illite/mica. This condition, along with the presence of traces of gehlenite, would suggest EFTs between 950 and 1050 °C.

AM4 is an overfired waste object that experimented EFTs higher than 1050 °C as suggested by the continuous vitrification and absence of illite/mica (Table 3; Fig. 7i); shift to reducing conditions of firing were also probable for the grayish color of the paste and absence of hematite.

AM5 is a grayish-black object that likely experienced reducing firing conditions, which show initial vitrification. For this specimen EFTs of 750–850 °C were inferred.

By estimating EFTs, a very interesting aspect emerged, namely that samples produced in the earlier period (6th-5th century BCE) show higher equivalent firing temperatures than those of the later period (4th-1st century BCE). Considering the concept of equivalent firing temperature (EFT; see De Bonis et al., 2017 and references therein for details), the actual temperatures reached in the kiln could have been higher than those to which the detected minerals decompose, as thickness and/or short firing duration cause a shift of decomposition reactions to higher temperatures (De Bonis et al., 2014). A relatively short firing duration and uncontrolled firing atmosphere with shift to reducing conditions (Maniatis and Tite, 1981) could be supposed as testified by samples FP7 and FP16 ascribed to the later period, spotted locally by an extensive vitrification with fine bloating pores.

The technological shift in the production of architectural terracotta could reflect a speeding up of the production due to a greater demand for material triggered by a construction surge in the frame of extensive political, economic, and social changes during the transition from the 5th to the 4th century BCE.

5. Conclusions

This study meticulously examined twenty-five fragments of architectural terracotta, ceramics and waste materials, carefully selected in a chronological span from the 6th century BCE to the 1st century BCE. The samples were collected from the *Fondo Patturelli* extra-urban sanctuary and from the *Alveo Marotta* furnace.

The petrographic approach revealed that all samples are characterized by fine inclusions of quartz and mica as a natural skeleton of the raw clay and a purposely added volcanic temper including sanidine, bytownite, diopside, trachyte lithics, and juvenile volcanic fragments (pumices and obsidians). The latter show a limited variability between trachyandesite-trachyte and tephriphonolite-phonolite composition, which is consistent with the products of the major Campanian eruptions. A distinction in three groups was made based on slight petrographic differences: the first group consists of 20 samples characterized by a larger amount of temper (25–30 %); the second group includes 2 samples from *Alveo Marotta* (AM1 and AM2), which differs for a lower percentage of inclusions (10–15 %); the third group is composed of 3 samples (AM3, AM5 from *Alveo Marotta* and FP14 from *Fondo Patturelli*) that are characterized by the presence of garnet showing the typical composition of the garnets (andradite-grossular) present in the Somma-Vesuvius products (i.e., Avellino pumice eruption).

Despite the petrographic differences, the multi-proxy approach revealed that the calcareous composition (CaO > 6 wt.%) of the clay raw material was a prevalent feature of the majority of the samples and of all architectural terracotta. Notably, among the potential sources of raw materials, locally derived Ca-rich clays from the Volturno River floodplain mixed with a volcanic temper typical from the investigated area were possibly exploited. In contrast, two samples (AM3 and AM5) exhibit a Ca-poor character (less than 6 wt.%), which is more compatible with the use of alluvial clays with a low calcium oxide concentration influenced by a pyroclastic component that also occur in this floodplain

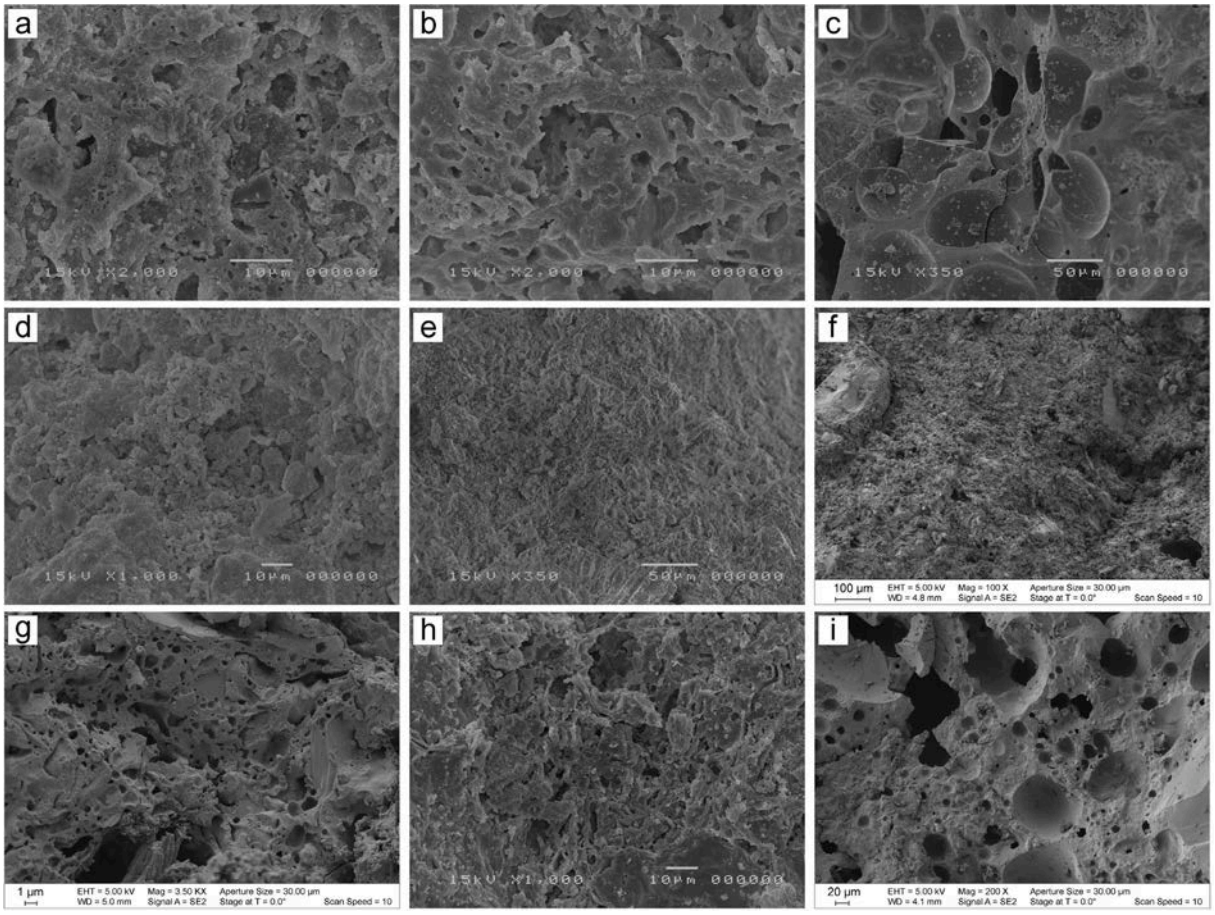

Fig. 7. SEM and FESEM* micrographs depicting the microstructure on freshly fractured sample surfaces: (a) FP17, initial vitrification/extensive vitrification (IV/V); (b) FP19, extensive vitrification (V); (c) FP6, continuous vitrification with coarse bloating pores CV(CB); (d) FP13, no vitrification (NV); (e) FP20, intermediate structure between no vitrification and initial vitrification (NV +); (f) FP7, initial vitrification (IV)*; (g) FP7, parts of the paste showing extensive vitrification with fine bloating pores*; (h) FP9, initial vitrification (IV); (i) AM4, continuous vitrification with coarse bloating pores CV(CB)*.

(see De Bonis et al., 2013; Verde et al., 2023b for details). This aspect is similar to what was hypothesized for the common wares and thin-walled pottery produced in the nearby sites of Cales (Verde et al., 2023b) and Alife (Grifa et al., 2015).

Although the samples were produced over an extremely wide time span, the production tradition of these roof tiles, and thus also the source of raw materials, remains the same, denoting a reliance on the use of the same recipes. The results obtained emphasize that the clay for the production of roof tiles in Capua was consistently sourced from the surrounding areas in the Volturno River floodplain (e.g., Pontelatone and Piana di Monte Verna), regardless of the political rule. This consistency in raw material sourcing and processing indicates a remarkable tradition that has persisted over generations. It highlights a deep-rooted commitment to preserving the craftsmanship and recipes used in creating these terracottas and ceramics, which withstood the test of time attesting to their enduring quality and heritage.

Focusing on firing temperatures, the examined architectural terracotta and ceramic samples generally exhibited two different firing modalities depending on the production period. In particular, samples of the earlier period (6th-5th century BCE) are characterized by equivalent firing temperatures ranging from 800 to over 1000 °C, whereas samples from the later period (4th-1st century BCE) exhibited lower equivalent firing temperatures, typically falling between < 750 to 850 °C. Similar low firing temperatures were also estimated by Russo et al. (2022) for roof tiles from the Heracles Sanctuary in Alba Fucens located just over a hundred km north-west in central Italy and ascribed to a comparable chronological interval (3rd to 2nd centuries BCE). Consequently, various hypotheses can be formulated to explain this phenomenon.

In the 4th century BCE, the once Etruscan city of Capua was under the hegemony of the Samnites. This period was marked by extensive political, economic, and social changes. Based on the city's phase plans, as compiled by N. Wagner (in press), a construction surge in Capua can be observed from the mid-4th century BCE and particularly in the 2nd century BCE. Not only this affected the archaic roofs of extramural sanctuaries like *Fondo Patturelli*, *Via Campania*, or *Diana Tifatina*, but the entire city experienced growth. More private and public buildings were erected and Capua became renowned for its ceramic, perfume, and bronze productions.

These developments could have influenced changes in the manufacture and design of roof tiles. Due to the increased demand for building materials and the intensified construction activity, it is possible to assume that the production of roof tiles was expedited. As a matter of fact, a long-lasting firing, possibly associated to high temperatures, would have required more time and fuel, such as wood. Due to the rising construction surge between the 4th and 2nd centuries BCE, time could not be wasted and, probably, wood was in high demand both as a fuel for kilns and as a construction material.

It is worth noting that not only in Capua but throughout Italy, sanctuaries were being renovated or newly constructed (Känel, 2001). Therefore, the question could also arise in other cases (e.g., Heracles Sanctuary in Alba Fucens), in which a production dynamic similar to that of the later period in Capua may have been adopted. Namely, to save time and materials. However, further research and investigations are required to fully understand the precise relationships and influences

of these events on roof tile production.

CRediT authorship contribution statement

Maria Verde: Writing – review & editing, Writing – original draft, Visualization, Methodology, Investigation, Formal analysis, Data curation, Conceptualization. **Alberto De Bonis:** Writing – review & editing, Writing – original draft, Visualization, Methodology, Investigation, Funding acquisition, Formal analysis, Data curation, Conceptualization. **Natalie Wagner:** Writing – original draft, Resources, Investigation, Formal analysis, Data curation, Conceptualization. **Francesca d'Aniello:** Writing – original draft, Formal analysis, Conceptualization. **Vincenzo Morra:** Writing – review & editing, Writing – original draft, Validation, Supervision, Methodology, Investigation, Funding acquisition.

Declaration of competing interest

The authors declare that they have no known competing financial interests or personal relationships that could have appeared to influence the work reported in this paper.

Data availability

Data will be made available on request.

Acknowledgments

This work was supported by funds from the DiSTAR (Vincenzo Morra and Alberto De Bonis) of the University of Naples Federico II. The authors wish to thank Ciro Cucciniello for high quality XRF analyses, Sergio Bravi for his technical ability in thin section preparation, and Roberto de Gennaro for his valuable support during FESEM and FESEM-EDS analysis.

The authors wish to thank Gennaro Leva, Soprintendente Archeologia belle arti e paesaggio per le province di Caserta e Benevento, Antonella Tomeo, Soprintendenza Archeologia belle arti e paesaggio per le province di Caserta e Benevento; Ida Gennarelli, Museo Archeologico dell'Antica Capua (MAAC) e Mitreo e dell'Anfiteatro Campano di Santa Maria Capua Vetere and Carlo Rescigno, Università degli Studi della Campania Luigi Vanvitelli, Dipartimento di Lettere e Beni Culturali (DiLBEC). The authors also wish to thank the craftsmen of the traditional brick workshop Fornace Saputo in Casapulla (Caserta) for providing technical support and information about use of local raw materials in the traditional production of bricks. The authors warmly thank Renata d'Aniello for the English revision of the manuscript, along with the Editor and two anonymous reviewers, who definitely improved the manuscript with their suggestions and comments.

Appendix A. Supplementary data

Supplementary material associated with this article can be found in the online version. Table S1: Composition of feldspars micro-analyzed via FESEM-EDS (wt.%) in the investigated architectural terracotta and ceramics; Table S2: Composition of pyroxenes micro-analyzed via FESEM-EDS (wt.%) in the investigated architectural terracotta and ceramics; Table S3: Composition of volcanic glass fragments micro-analysed via FESEM-EDS (wt.%) in the investigated architectural terracotta and ceramics. Values given are normalized to 100%; Table S4: Raw materials and modern brick samples used for the chemical comparison with their high-CaO (HCC, CaO > 6%) and low-CaO (LCC, CaO < 6%) character. Geological information is from Vitale and Ciarcia (2018); Table S5: Bulk chemical composition raw materials and modern brick samples analyzed by X-ray fluorescence used for chemical comparison. Major oxides (wt.%) are L.O.I. free. Trace elements are expressed in ppm (parts per million); Table S6: Composition of garnets micro-analyzed via FESEM-EDS (wt.%) in the investigated architectural terracotta and ceramics. End-members are calculated from Locock (2008). Supplementary data to this article can be found online at https://doi.org/10.1016/j.jasrep.2024.104708.

References

Allegro, N., 1984. Insediamento arcaico e necropoli sannitica presso l'Alveo Marotta. Studi Etruschi LII 514–517.
Allegro, N., Svanera, S., 1996. Santa Maria Capua Vetere (Caserta). Proprietà Merola. Campagne di scavo 1996–1997, Bollettino di Archeologia 37/38, 83-87.
Ascione, A., Ciarcia, S., Di Donato, V., Mazzoli, S., Vitale, S., 2012. The Pliocene-Quaternary wedge-top basins of southern Italy: An expression of propagating lateral slab tear beneath the Apennines. Basin Res. 24, 456–474.
Cerchiai, L., 1995. Gli antichi popoli della Campania. Milan, Italy, Carocci, pp. 1–151.
Ciarcia, S., Vitale, S., 2013. Sedimentology, stratigraphy and tectonics of evolving wedge-top depozone: Ariano Basin, southern Apennines, Italy. Sediment. Geol. 290, 27–46.
Cucciniello, C., Melluso, L., le Roex, A.P., Jourdan, F., Morra, V., de' Gennaro, R., Grifa, C., 2017. From nephelinite, basanite and basalt to peralkaline trachyphonolite and comendite in the Ankaratra volcanic complex, Madagascar: 40Ar/39Ar ages, phase compositions and bulk-rock geochemical and isotopic evolution. Lithos 274–275, 363–382. https://doi.org/10.1306/74D70466-2B21-11D7-8648000102C1865D.
Cultrone, G., Rodríguez-Navarro, C., Sebastián, E., 2001. Carbonate and silicate phase reactions during ceramic firing. Eur. J. Miner. 13, 621–634. https://doi.org/10.1127/0935-1221/2001/0013-0621.
D'Argenio, B., Barattolo, F. Budillon, F., Cesarano, M., Donadio, C., Pappone, G., Pugliese, A., Putignano, M.L., Aucelli, P.P.C., Russo Ermolli, E., Sgrosso, A. Terlizzi, F., Ferrari, G., Lamagna, R., 2012. Carta Geologica della Regione Campania, Note Illustrative della Carta Geologica 191 alla scala 1: 10.000, Foglio 484 Isola di Capri, Regione Campania – Assessorato Difesa del Suolo.
De Bonis, A., Grifa, C., Cultrone, G., De Vita, P., Langella, A., Morra, V., 2013. Raw materials for archaeological pottery from the Campania region of Italy: a petrophysical characterization. Geoarchaeology 28 (5), 478–503. https://doi.org/10.1002/gea.21450.
De Bonis, A., Cultrone, G., Grifa, C., Langella, A., Morra, V., 2014. Clays from the Bay of Naples (Italy): New insight on ancient and traditional ceramics. J. Eur. Ceram. Soc. 34, 3229–3244. https://doi.org/10.1016/j.jeurceramsoc.2014.04.014.
De Bonis, A., Febbraro, S., Germinario, C., Giampaola, D., Grifa, C., Guarino, V., Langella, A., Morra, V., 2016. Distinctive volcanic material for the production of campana a ware: the workshop area of Neapolis at the Duomo Metro Station in Naples. Italy. Geoarchaeology 31 (6), 437–466. https://doi.org/10.1002/gea.21571.
De Bonis, A., D'Angelo, M., Guarino, V., Massa, S., Anaraki, F.S., Genito, B., Morra, V., 2017. Unglazed pottery from the masjed-i jom'e of Isfahan (Iran): technology and provenance. Archaeol. Anthropol. Sci. 9, 617–635. https://doi.org/10.1007/s12520-016-0407-z.
Di Girolamo, P., Stanzione, D., 1973. Lineamenti geologici e petrologici dell'isola di Procida. Rend. Soc. Ital. Min. Petrol. 29, 81–126.
Fedele, L., Insinga, D., Calvert, A.T., Morra, V., Perrotta, A., Scarpati, C., 2011. 40 Ar/39 Ar dating of tuff vents in the Campi Flegrei caldera (southern Italy): toward a new chronostratigraphic reconstruction of the Holocene volcanic activity. Bull. Volcanol. 73, 1323–1336.
Fedele, L., 2022. An Evolutionary Model for the Magmatic System of the Campi Flegrei Volcanic Field (Italy) Constrained by Petrochemical Data. In: G. Orsi, M. D'Antonio, L. Civetta (Eds.), Campi Flegrei: A Restless Caldera in a Densely Populated Area, Berlin, Heidelberg: Springer Berlin Heidelberg, pp. 95-123.
Franchi De Bellis, A., 1981. Le iovile capuane, first ed. L.S. Olschki, Florence, Italy, pp. 1–238.
Grifa, C., De Bonis, A., Guarino, V., Petrone, C.M., Germinario, C., Mercurio, M., Soricelli, G., Langella, A., Morra, V., 2015. Thin walled pottery from Alife (Northern Campania, Italy). Period. Mineral. 84, 65–90. https://doi.org/10.2451/2015PM0005.
Guarino, V., De Bonis, A., Grifa, C., Langella, A., Morra, V., Pedroni, L., 2011. Archaeometric study on terra sigillata from Cales (Italy). Period. Mineral. 80, 455–470. https://doi.org/10.2451/2011PM0030.
Guarino, V., De Bonis, A., Peña, J.T., Verde, M., Morra, V., 2021a. Multianalytical investigation of wasters from the Tower 8/Porta di Nola refuse middens in Pompeii: Sr–Nd isotopic, chemical, petrographic, and mineralogical analyses. Geoarcheaology 36, 712–739. https://doi.org/10.1306/74D70466-2B21-11D7-8648000102C1865D.
Guarino, V., Lustrino, M., Zanetti, A., Tassinari, C.C., Ruberti, E., de' Gennaro, R., Melluso, L., 2021b. Mineralogy and geochemistry of a giant agpaitic magma reservoir: the Late Cretaceous Poços de Caldas potassic alkaline complex (SE Brazil). Lithos 398, 106330. https://doi.org/10.1306/74D70466-2B21-11D7-8648000102C1865D.
Haase, U., 2020. Zwischen Tradition und Rezeption: Die matronalen Sitzstatuen aus dem Fundkontext Fondo Patturelli (Capua), pp. 1-324, https://kups.ub.uni-koeln.de/11606/.
Känel, R., 2001. Bilderzyklen aus Terrakotta. Untersuchungen zur etruskisch-italischen Baudekoration des 3. und 2. Jahrhunderts v. Chr., 1st ed., Universität: Munich, Germany, 1-319.
Koch, H., 1907. Hellenistische Architekturstücke in Capua. In Mitteilungen Des Deutschen Archäologischen Instituts, Römische Abteilung 22, 61–428.

Koch, H., 1912. Dachterrakotten aus Campanien mit Ausschluss von Pompei, first ed. Berlin, Germany, Reimer, pp. 1–99.

Le Bas, M., Rex, D., Stillman, C., 1986. The early magmatic chronology of Fuerteventura, Canary Islands. Geol. Mag. 123 (3), 287–298. https://doi.org/10.1017/S0016756800034762.

Locock, A.J., 2008. An Excel spreadsheet to recast analyses of garnet into end-member components, and a synopsis of the crystal chemistry of natural silicate garnets. Computers & Geosciences 34, 1769–1780.

Maniatis, Y., Tite, M.S., 1981. Technological examination of Neolithic-Bronze Age pottery from central and southeast Europe and from the Near East. J. Archaeol. Sci. 8, 59–76. https://doi.org/10.1306/74D70466-2B21-11D7-8648000102C1865D.

Melluso, L., de' Gennaro, R., Fedele, L., Franciosi, L., Morra, V., 2012. Evidence of crystallization in residual, Cl–F-rich, agpaitic, trachyphonolitic magmas and primitive Mg-rich basalt–trachyphonolite interaction in the lava domes of the Phlegrean Fields (Italy). Geol. Mag. 149 (3), 532–550.

Melluso, L., Scarpati, C., Zanetti, A., Sparice, D., de' Gennaro, R., 2022. The petrogenesis of chemically zoned, phonolitic, Plinian and sub-Plinian eruptions of Somma-Vesuvius, Italy: Role of accessory phase removal, independently filled magma reservoirs with time, and transition from slightly to highly silica undersaturated magmatic series in an ultrapotassic stratovolcano. Lithos 430, 106854.

Migliore, R.P., 2011. Statuine votive dal santuario del fondo Patturelli. Una proposta di lettura. In: O., Paoletti, M.C., Bettini, (Eds.), Gli Etruschi e la Campania settentrionale. Proceedings of XXVI convegno di Studi Etruschi ed Italici, Caserta, Santa Maria Capua Vetere, Capua Teano, Italy, November 11th-15th 2007, Serra: Pisa, Italy, pp. 409-417.

Minoja, M., 2006. "Ciotola di forma insolita". Una nuova forma ceramica delle fasi iniziale del fondo patturelli a Capua. In: Studi di protostoria in onore di Renato Peroni. All'Insegna del Giglio: Borgo di San Lorenzo, Italy, pp. 650-656.

Morra, V., Calcaterra, D., Cappelletti, P., Colella, A., Fedele, L., De'Gennaro, R., Langella, A., Mercurio, M., et al., 2010. Urban geology: relationships between geological setting and architectural heritage of the Neapolitan area. J. Virtual Explor. 36 (27) https://doi.org/10.3809/jvirtex.2010.00261.

Nodari, L., Marcuz, E., Maritan, L., Mazzoli, C., Russo, U., 2007. Hematite nucleation and growth in the firing of carbonate-rich clay for pottery production. J. Eur. Ceram. Soc. 27, 4665–4673. https://doi.org/10.1016/j.jeurceramsoc.2007.03.031.

Petrillo, N., 2016. Matres capuane e kourotrophia. Qualche Nuova Considerazione Iconografica, Oebalus, Studi Sulla Campania Nell'antichità 11, 375–389.

Quinn, S.P., 2013. Ceramic petrography: the interpretation of archaeological pottery & related artefacts in thin section. Archaeopress, Oxford. Doi: 10.2307/j.ctv1jk0jf4.

Rescigno, C., Sampaolo, V., 2005. Appunti sull'impiego del colore sulle terrecotte architettoniche capuane. Mediterranea II, 133–163.

Rescigno, C., 2009. Un bosco di madri. Il santuario di Fondo Patturelli tra documenti e contesti. In: M.L., Chirico, R., Cioffi, G., Pignatelli Spinazzola, S., Quilici Gigli (Eds.), Lungo l'Appia. Scritti su Capua antica e dintorni, Chirico, Giannini Editore, Naples, Italy, pp. 31-42.

Rispoli, C., De Bonis, A., Guarino, V., Graziano, S.F., Di Benedetto, C., Esposito, R., Morra, V., Cappelletti, P., 2019. The ancient pozzolanic mortars of the Thermal complex of Baia (Campi Flegrei, Italy). J. Cult. Herit. 40, 143–154. https://doi.org/10.1306/74D70466-2B21-11D7-8648000102C1865D.

Rolandi, G., Bellucci, F., Heizler, M.T., Belkin, H.E., De Vivo, B., 2003. Tectonic controls on the genesis of ignimbrites from the Campanian Volcanic Zone, southern Italy. Mineral Petrol 79, 3–31.

Russo, G., Ceccaroni, E., Conte, A.M., Medeghini, L., De Vito, C., Mignardi, S., 2022. Archaeometric Study on Roman Painted Terracottas from the Sanctuary of Hercules in Alba Fucens (Abruzzo, Italy). Minerals 12, 346. https://doi.org/10.3390/min12030346.

Sampaolo, V., 2011. I nuovi scavi fondo Patturelli. Elementi per una definizione topografica Culture a contatto in Campania, Processi di trasformazione tra V e IV secolo a.C. Annali Della Facoltà Di Lettere e Filosofia Dell'università Degli Studi Di Milano 64, 6–20.

Scheibner, B., Wörner, G., Civetta, L., Stosch, H.G., Simon, K., Kronz, A., 2007. Rare earth element fractionation in magmatic Ca-rich garnets. Contrib. Mineral. Petrol. 154, 55–74. https://doi.org/10.1007/s00410-006-0179-z.

Sulpizio, R., Cioni, R., Di Vito, M.A., Mele, D., Bonasia, R., Dellino, P., 2010. The Pomici di Avellino eruption of Somma-Vesuvius (3.9 ka BP). Part I: stratigraphy, compositional variability and eruptive dynamics. Bull. Volcanol. 72, 539–558. https://doi.org/10.1007/s00445-010-0379-2.

Terry, R.D., Chilingar, G.V., 1995. Summary of "Concerning some additional aids in studying sedimentary formations," by MS J. Shvetsov. Sediment. Res. 25, 229–234. https://doi.org/10.1306/74D70466-2B21-11D7-8648000102C1865D.

Verde, M., De Bonis, A., Renson, V., Germinario, C., Rispoli, C., D'Uva, F., Tomeo, A., Morra, V., 2023a. Minero-petrographic characterization of fine ware from Cales (South Italy). Archaeometry 65, 1145–1184. https://doi.org/10.1111/arcm.12873.

Verde, M., De Bonis, A., Tomeo, A., Renson, V., Germinario, C., D'Uva, F., Rispoli, C., Morra, V., 2023b. Differently Calenian: A multi-analytical approach for the characterization of coarse ware from Cales (South Italy). J. Archaeol. Sci. Rep. 49, 103941 https://doi.org/10.1016/j.jasrep.2023.103941.

Vincenzini, P., Fiori, C., 1977. Caratteristiche naturali di argille italiane e correlazione con le proprietà tecnologiche dei prodotti da esse ottenibili. Ceramurgia 3, 119–134.

Vitale, S., Ciarcia, S., 2018. Tectono-stratigraphic setting of the Campania region (southern Italy). J. Maps 14 (2), 9–21.

Wagner, N., in press. Coroplastica Campana. Le terrecotte architettoniche di Capua dal IV secolo a.C. al I d.C.

Whitbread, I.K., 1995. Greek transport amphorae: a petrological and archaeological study. Fitch Laboratory Occasional Paper, 4. British School at Athens.

Williams, D. F., 1990. The study of ancient ceramics: the contribution of the petrographic method. In Scienze in archeologia. Quaderni del Dipartimento di Archeologia e Storia delle Arti, Università di Siena, Mannoni, T., Molinari, A., All'insegna del Giglio: Firenze, Italy, pp. 43–64.

Wolf, M., 2023. Zweiter Teil: Hellenistische Altäre vom Fondo Patturelli in Capua. In Hellenistische Heiligtümer in Kampanien. Sakralarchitektur im Grenzgebiet zwischen Großgriechenland und Rom, Wolf, M., Harrassowitz Verlag, Wiesbaden, Germany, pp. 11-14.